Author(s): Tuovinen, Toni & Hinkkanen, Marko & Luomi, Jorma

Title: A comparison of an adaptive full-order observer and a reduced-order observer for synchronous reluctance motor drives

Year: 2011

Version: Post print

Please cite the original version:

Tuovinen, Toni & Hinkkanen, Marko & Luomi, Jorma. 2011. A comparison of an adaptive full-order observer and a reduced-order observer for synchronous reluctance motor drives. 2011 Symposium on Sensorless Control for Electrical Drives (SLED). 5. ISBN 978-1-4577-1853-3 (electronic). DOI: 10.1109/sled.2011.6051555.

A Comparison of an Adaptive Full-Order Observer and a Reduced-Order Observer for Synchronous Reluctance Motor Drives

Toni Tuovinen, Marko Hinkkanen, and Jorma Luomi
Aalto University School of Electrical Engineering
Department of Electrical Engineering, P.O. Box 13000, FI-00076 Aalto, Finland

***Abstract*—Two back-EMF-based position observers are compared for motion-sensorless synchronous reluctance motor drives. The reduced-order observer is of the second order, and the adaptive full-order observer is of the fourth order. The proposed design rules guarantee the stability of the adaptive full-order observer, if the parameter estimates are accurate. The observers are experimentally evaluated using a 6.7-kW synchronous reluctance motor drive in low-speed operation and under parameter errors. The gain selection of the second-order observer is easier, but the adaptive full-order observer is more robust against parameter variations and spatial harmonics.**

***Index Terms*—Observer, stability conditions, speed sensorless, parameter uncertainties.**

I. Introduction

Modern synchronous reluctance motors (SyRMs) are becoming interesting competitors to induction motors and permanent-magnet synchronous motors in variable-speed drives [1], [2]. The rotor position of a synchronous motor has to be known with good accuracy in order to obtain stable operation and high performance. The rotor position can be either measured or estimated. Motion-sensorless control based on position estimation is usually preferable: motion sensors are expensive, they can be damaged or, in some environments and applications, cannot be installed.

Position estimation methods based on signal injection can be used for SyRMs. In order to avoid additional noise and losses, it is desirable to use a method based on the back electromotive force (EMF), and combine a signal-injection method with it only at the lowest speeds [3], [4]. Since SyRMs are closely related to permanent-magnet synchronous motors (PMSMs), back-EMF based estimation methods proposed for PMSMs, for example the observers proposed in [5], [6] and [7], can be used for SyRMs with slight modifications.

The gain selection of back-EMF-based observers is crucial in order to obtain good performance and robustness against measurement errors and parameter variations. As the order of the observer increases, the analysis becomes increasingly complicated, and it might be difficult to derive the stability conditions even if the parameter estimates are accurate. Hence, a low-order observer is an attractive design goal.

In this paper, two different observers are compared using a 6.7-kW SyRM drive. The reduced-order observer is of the second order, and the adaptive full-order observer is of the fourth order. For the adaptive full-order observer, design rules are proposed, simplifying the stability analysis. The properties evaluated experimentally are the sensitivity to parameter uncertainties, sensitivity to harmonic noise, behavior during load transients, and stability in low-speed operation.

II. SyRM Model and Rotor-Position Observers

A. Model

Real space vectors will be used here. For example, the stator-current vector is $\boldsymbol{i}_\mathrm{s} = [i_\mathrm{d}, i_\mathrm{q}]^\mathrm{T}$, where i_d and i_q are the components of the vector and the matrix transpose is marked with the superscript T. The orthogonal rotation matrix is defined as

$$\mathbf{J} = \begin{bmatrix} 0 & -1 \\ 1 & 0 \end{bmatrix}.$$

The electrical position of the d axis is denoted by ϑ_m. The d axis is defined as the direction of the maximum inductance of the rotor. The position depends on the electrical angular rotor speed ω_m according to

$$\frac{\mathrm{d}\vartheta_\mathrm{m}}{\mathrm{d}t} = \omega_\mathrm{m} \tag{1a}$$

To simplify the analysis in the following sections, the machine model will be expressed in the *estimated* rotor reference frame, whose d axis is aligned at $\hat{\vartheta}_\mathrm{m}$ with respect to the stator reference frame. The stator inductance is

$$\boldsymbol{L} = \mathrm{e}^{-\tilde{\vartheta}_\mathrm{m}\mathbf{J}} \begin{bmatrix} L_\mathrm{d} & 0 \\ 0 & L_\mathrm{q} \end{bmatrix} \mathrm{e}^{\tilde{\vartheta}_\mathrm{m}\mathbf{J}} \tag{1b}$$

where $\tilde{\vartheta}_\mathrm{m} = \hat{\vartheta}_\mathrm{m} - \vartheta_\mathrm{m}$ is the estimation error in the rotor position, L_d the direct-axis inductance, and L_q the quadrature-axis inductance. The voltage equation is

$$\frac{\mathrm{d}\boldsymbol{\psi}_\mathrm{s}}{\mathrm{d}t} = \boldsymbol{u}_\mathrm{s} - R_\mathrm{s}\boldsymbol{i}_\mathrm{s} - \hat{\omega}_\mathrm{m}\mathbf{J}\boldsymbol{\psi}_\mathrm{s} \tag{1c}$$

where $\boldsymbol{\psi}_\mathrm{s}$ is the stator-flux vector, $\boldsymbol{u}_\mathrm{s}$ the stator-voltage vector, R_s the stator resistance, and $\hat{\omega}_\mathrm{m} = \mathrm{d}\hat{\vartheta}_\mathrm{m}/\mathrm{d}t$ is the angular speed of the coordinate system. The stator current is a nonlinear function

$$\boldsymbol{i}_\mathrm{s} = \boldsymbol{L}^{-1}\boldsymbol{\psi}_\mathrm{s} \tag{1d}$$

of the stator-flux vector and the position error $\tilde{\vartheta}_\mathrm{m}$.

B. Reduced-Order Observer

The reduced-order observer proposed in [7] is considered. It is based on estimating the rotor position and the d component $\hat{\psi}_\mathrm{d}$ of the stator flux in the estimated rotor coordinates. For a SyRM, the componentwise presentation of the observer is

$$\frac{\mathrm{d}\hat{\psi}_\mathrm{d}}{\mathrm{d}t} = u_\mathrm{d} - \hat{R}_\mathrm{s} i_\mathrm{d} + \hat{\omega}_\mathrm{m}\hat{L}_\mathrm{q} i_\mathrm{q} + k_1(\hat{\psi}_\mathrm{d} - \hat{L}_\mathrm{d} i_\mathrm{d}) \tag{2a}$$

$$\frac{\mathrm{d}\hat{\vartheta}_\mathrm{m}}{\mathrm{d}t} = \frac{u_\mathrm{q} - \hat{R}_\mathrm{s} i_\mathrm{q} - \hat{L}_\mathrm{q}\frac{\mathrm{d}i_\mathrm{q}}{\mathrm{d}t} + k_2(\hat{\psi}_\mathrm{d} - \hat{L}_\mathrm{d} i_\mathrm{d})}{\hat{\psi}_\mathrm{d}} \tag{2b}$$

where $\hat{L}_\mathrm{d}$ and $\hat{L}_\mathrm{q}$ are the estimated d and q axis inductances, respectively, $\hat{R}_\mathrm{s}$ is the estimated stator resistance, and k_1 and k_2 are the observer gains. The observer is of the second order, and there are only two gains.

With accurate parameter estimates, the closed-loop system consisting of (1) and (2) is locally stable in every operating point if the gains are given by

$$k_1 = -\frac{b + \beta(c/\hat{\omega}_\mathrm{m} - \hat{\omega}_\mathrm{m})}{\beta^2 + 1}, \quad k_2 = \frac{\beta b - c/\hat{\omega}_\mathrm{m} + \hat{\omega}_\mathrm{m}}{\beta^2 + 1} \tag{3}$$

where $\beta = i_\mathrm{q}/i_\mathrm{d}$, and the design parameters $b > 0$ and $c > 0$ may depend on the operating point [7]. The parameters b and c are actually the coefficients of the characteristic polynomial, $s^2 + bs + c$, of the linearized system consisting of (1) and (2). The relation between the two design parameters for the reduced-order observer is chosen as

$$c = \sqrt{3} b |\hat{\omega}_\mathrm{m}| + \hat{\omega}_\mathrm{m}^2 \tag{4}$$

which guarantees maximum robustness against parameter errors in low-speed operation [8].

C. Adaptive Full-Order Observer

In the adaptive full-order observer [5], [6], both stator-flux vector components are estimated,

$$\frac{\mathrm{d}\hat{\boldsymbol{\psi}}_\mathrm{s}}{\mathrm{d}t} = \boldsymbol{u}_\mathrm{s} - \hat{R}_\mathrm{s}\hat{\boldsymbol{i}}_\mathrm{s} - \hat{\omega}_\mathrm{m}\mathbf{J}\hat{\boldsymbol{\psi}}_\mathrm{s} - \boldsymbol{K}\tilde{\boldsymbol{i}}_\mathrm{s} \tag{5a}$$

$$\hat{\boldsymbol{i}}_\mathrm{s} = \hat{\boldsymbol{L}}^{-1}\hat{\boldsymbol{\psi}}_\mathrm{s} \tag{5b}$$

where $\hat{\boldsymbol{i}}_\mathrm{s}$ is the estimated stator-current vector, the estimation error of the stator current is $\tilde{\boldsymbol{i}}_\mathrm{s} = \hat{\boldsymbol{i}}_\mathrm{s} - \boldsymbol{i}_\mathrm{s}$ and $\boldsymbol{K}$ is the gain matrix.

The rotor speed is estimated with the PI mechanism

$$\hat{\omega}_\mathrm{m} = \boldsymbol{k}_\mathrm{p}\tilde{\boldsymbol{i}}_\mathrm{s} + \boldsymbol{k}_\mathrm{i}\int \tilde{\boldsymbol{i}}_\mathrm{s} dt \tag{6}$$

The gain vectors $\boldsymbol{k}_\mathrm{p}$ and $\boldsymbol{k}_\mathrm{i}$ are chosen to utilize the estimation error only in the q axis direction,

$$\boldsymbol{k}_\mathrm{p} = [0, k_\mathrm{p}], \quad \boldsymbol{k}_\mathrm{i} = [0, k_\mathrm{i}] \tag{7}$$

The proposed gain matrix is

$$\boldsymbol{K} = \begin{bmatrix} -\hat{L}_\mathrm{d} k_1 - \hat{R}_\mathrm{s} & \hat{L}_\mathrm{q}\beta k_1 \\ -\hat{L}_\mathrm{d} k_2 & \hat{L}_\mathrm{q}\beta k_2 - \hat{R}_\mathrm{s} \end{bmatrix} \tag{8}$$

where k_1 and k_2 are given by (3). For convenience, the gains k_p and k_i are selected according to

$$k_\mathrm{p} = \frac{\hat{L}_\mathrm{q} d}{(\hat{L}_\mathrm{d} - \hat{L}_\mathrm{q}) i_\mathrm{d}} \tag{9a}$$

$$k_\mathrm{i} = \frac{\hat{L}_\mathrm{q} e}{(\hat{L}_\mathrm{d} - \hat{L}_\mathrm{q}) i_\mathrm{d}} \tag{9b}$$

where d and e are design parameters, which may depend on the rotor speed. With this gain selection, the characteristic polynomial of the closed-loop system consisting of (1), (5), (6), (7), (8) and (9) can, after linearization, be split into a product of two second-order polynomials,

$$(s^2 + bs + c)(s^2 + ds + e) \tag{10}$$

and the stability is guaranteed for all positive values of b, c, d and e, if the parameter estimates are accurate. The observer is of the fourth order, and there are four gains. It can be seen that the characteristic polynomial (10) is closely related to the reduced-order observer, since the characteristic polynomial of the reduced-order observer is $s^2 + bs + c$.

The proposed observer design is a subset of all stable design possibilities, since the gain matrix (8) has only two free parameters instead of four. With the proposed design, however, the stability analysis based on (10) is considerably simpler than that of a more general fourth-order polynomial.

III. Experimental Setup and Parameters

The motion-sensorless control system was implemented in a dSPACE DS1104 PPC/DSP board. A 6.7-kW four-pole SyRM was fed by a frequency converter that is controlled by the DS1104 board. The rated values of the SyRM are: speed 3175 r/min; frequency 105.8 Hz; line-to-line rms voltage 370 V; rms current 15.5 A; and torque 20.1 Nm. The base values for angular speed, voltage, and current are defined as $2\pi \cdot 105.8$ rad/s, $\sqrt{2/3} \cdot 370$ V, and $\sqrt{2} \cdot 15.5$ A, respectively.

A servo motor was used as a loading machine. The rotor speed ω_m and position ϑ_m were measured using an incremental encoder for monitoring purposes. The shaft torque T_m was measured using a Dataflex 22 torque measuring shaft. The total moment of inertia of the experimental setup is 0.015 kgm^2 (2.7 times the inertia of the SyRM rotor).

The stator currents and the DC-link voltage were measured, and the reference voltage obtained from the current controller was used for the observer. The sampling was synchronized to the modulation, and both the switching frequency and the sampling frequency were 8 kHz. A simple current feedforward compensation for dead times and power device voltage drops was applied.

The control system was augmented with a speed controller, whose feedback signal was the speed estimate $\hat{\omega}_\mathrm{m}$ obtained from the proposed observer. The bandwidth of this PI controller, including active damping [9], was $2\pi \cdot 5.3$ rad/s (0.05 p.u.). The estimate of the per-unit electromagnetic torque was evaluated as $\hat{T}_\mathrm{e} = (L_\mathrm{d} - L_\mathrm{q}) i_\mathrm{d} i_\mathrm{q}$.

The gain values were chosen based on empirical results. The gain $b = 2$ was used for the reduced-order observer. For

TABLE I
PER-UNIT PARAMETERS FOR SATURATION MODEL

$L_{\rm d0}$	$L_{\rm q0}$	α	γ	δ	$i_{\rm d0}$	$i_{\rm q0}$
3.15	0.685	2.24	0.353	0.085	0.2	0.2

the adaptive full-order observer, the gains were: $b = 0.05$, $c = 0.025|\hat{\omega}_{\rm m}| + \hat{\omega}_{\rm m}^2$, $d = 2$ and $e = 1$.

The saturation has been modeled as functions of the measured current,

$$L_{\rm d} = \begin{cases} L_{\rm d0} - \alpha i_{\rm d} - \delta \left|\frac{i_{\rm q}}{i_{\rm d0}}\right|, & \text{if } i_{\rm d} \le i_{\rm d0} \\ L_{\rm d0} - \alpha i_{\rm d} - \delta \left|\frac{i_{\rm q}}{i_{\rm d}}\right|, & \text{otherwise} \end{cases} \tag{11a}$$

$$L_{\rm q} = \begin{cases} L_{\rm q0} - \gamma |i_{\rm q}| - \delta \left|\frac{i_{\rm d}}{i_{\rm q0}}\right|, & \text{if } i_{\rm q} \le i_{\rm q0} \\ L_{\rm q0} - \gamma |i_{\rm q}| - \delta \left|\frac{i_{\rm d}}{i_{\rm q}}\right|, & \text{otherwise} \end{cases} \tag{11b}$$

where $i_{\rm d0}$ and $i_{\rm q0}$ are transition values for $i_{\rm d}$ and $i_{\rm q}$ to avoid divisions by small numbers. The saturation model parameters are given in Table I. The estimated stator resistance is $\hat{R}_{\rm s} = 0.042$ p.u.

IV. EXPERIMENTAL RESULTS

Fig. 1 shows the effect of the parameter errors on the position estimation error at the speed $\hat{\omega}_{\rm m} = 0.1$ p.u. with 50% rated load torque applied. The reduced-order observer is used in Fig. 1(a), and the adaptive full-order observer is used in Fig. 1(b). The data is captured by varying each parameter estimate from 90% up to 110% of the actual value in 10 seconds. It can be seen that the model parameters $\hat{R}_{\rm s}$ and $\hat{L}_{\rm q}$ have only a small effect on the position error, whereas incorrect value for $\hat{L}_{\rm d}$ increases the estimation error rapidly in Fig. 1(a), when the reduced-order observer is used. According to Fig. 1(b), the adaptive full-order observer is less sensitive to parameter errors. It should be noted that the relative errors of $L_{\rm d}$ and $L_{\rm q}$ are defined with respect to the (original) operation point values. As the estimation error increases, the actual values of $i_{\rm d}$ and $i_{\rm q}$ change, resulting changes in actual values of $L_{\rm d}$ and $L_{\rm q}$ due to saturation.

Experimental results of a stepwise speed reversal from $\hat{\omega}_{\rm m} = 0.10$ p.u. to $\hat{\omega}_{\rm m} = -0.10$ p.u. and back to 0.10 p.u. with rated load torque applied are depicted in Fig. 2. The reduced-order observer is used in Fig. 2(a), and the adaptive full-order observer is used in Fig. 2(b). It can be seen that the reduced-order observer amplifies the estimation noise in the regenerating mode in Fig. 2(a). This behavior is analyzed in [8]. With the adaptive full-order observer, the amplitude of the estimation noise does not depend on the operating mode, as seen in Fig. 2(b).

When the reduced-order observer is used, spatial harmonics cause noise in the position estimate in the regenerating mode if the machine is highly saturated [8]. Results of a slow change of $i_{\rm d}$ from 0.3 p.u. to 0.5 p.u. with -50% rated load torque applied are shown in Fig. 3. The reduced-order observer is used in Fig. 3(a), and the adaptive full-order observer is used in Fig. 3(b). It can be seen that as $i_{\rm d}$ increases in the regenerating mode, the noise in the position estimate of the reduced-order observer increases, but the adaptive full-order observer is not sensitive to spatial harmonics.

Experimental results of load-torque steps when the speed reference was kept at 0.05 p.u. are shown in Fig. 4. The load torque was stepped to -75% of the rated load torque at $t = 2.5$ s, reversed at $t = 7.5$ s, and removed at $t = 12.5$ s. The reduced-order observer is used in Fig. 4(a), and the adaptive full-order observer is used in Fig. 4(b). It can be seen that the observers behave well in load transients in low-speed operation.

V. CONCLUSIONS

In this paper, two back-EMF-based observers are compared for synchronous reluctance motor drives. The gain selection of the observers is crucial in sustained low-speed operation. The analysis and tuning of the reduced-order observer is considerably easier than that of the adaptive full-order observer. The adaptive full-order observer has four design parameters, and the reduced-order observer has only one design parameter. The proposed design rules guarantee the stability of the adaptive full-order observer, if the parameter estimates are accurate. The experimental results indicate that the adaptive full-order observer is less sensitive to harmonic noise and parameter uncertainties than the reduced-order observer.

ACKNOWLEDGMENT

The authors gratefully acknowledge ABB Oy for the financial support.

REFERENCES

[1] E. Capecchi, P. Guglielmo, M. Pastorelli, and A. Vagati, "Position-sensorless control of the transverse-laminated synchronous reluctance motor," *IEEE Trans. Ind. Appl.*, vol. 37, no. 6, pp. 1768–1776, Nov./Dec. 2001.

[2] H. F. Hofmann, S. R. Sanders, and A. EL-Antably, "Stator-flux-oriented vector control of synchronous reluctance machines with maximized efficiency," *IEEE Trans. Ind. Electron.*, vol. 51, no. 5, pp. 1066–1072, Oct. 2004.

[3] A. Piippo, M. Hinkkanen, and J. Luomi, "Sensorless control of PMSM drives using a combination of voltage model and HF signal injection," in *Conf. Rec. IEEE-IAS Annu. Meeting*, vol. 2, Seattle, WA, Oct. 2004, pp. 964–970.

[4] O. Wallmark, L. Harnefors, and O. Carlson, "An improved speed and position estimator for salient permanent-magnet synchronous motors," *IEEE Trans. Ind. Electron.*, vol. 52, no. 1, pp. 255–262, Feb. 2005.

[5] G. Yang, R. Tomioka, M. Nakano, and T. H. Chin, "Position and speed sensorless control of brushless DC motor based on an adaptive observer," *IEEJ Trans. Ind. Appl.*, vol. 113, pp. 579–586, May 1993.

[6] A. Piippo, M. Hinkkanen, and J. Luomi, "Analysis of an adaptive observer for sensorless control of interior permanent magnet synchronous motors," *IEEE Trans. Ind. Electron.*, vol. 55, no. 2, pp. 570–576, Feb. 2008.

[7] M. Hinkkanen, T. Tuovinen, L. Harnefors, and J. Luomi, "A combined position and stator-resistance observer for salient PMSM drives: design and stability analysis," *IEEE Trans. Power Electron.*, no. 99, 2011, doi:10.1109/tpel.2011.2118232, in press.

[8] T. Tuovinen, M. Hinkkanen, and J. Luomi, "Analysis and design of a position observer with resistance adaptation for synchronous reluctance motor drives," in *Proc. IEEE ECCE'11*, Phoenix, AZ, Sep. 2011, in press.

[9] L. Harnefors, "Design and analysis of general rotor-flux-oriented vector control systems," *IEEE Trans. Ind. Electron.*, vol. 48, no. 2, pp. 383–390, Apr. 2001.

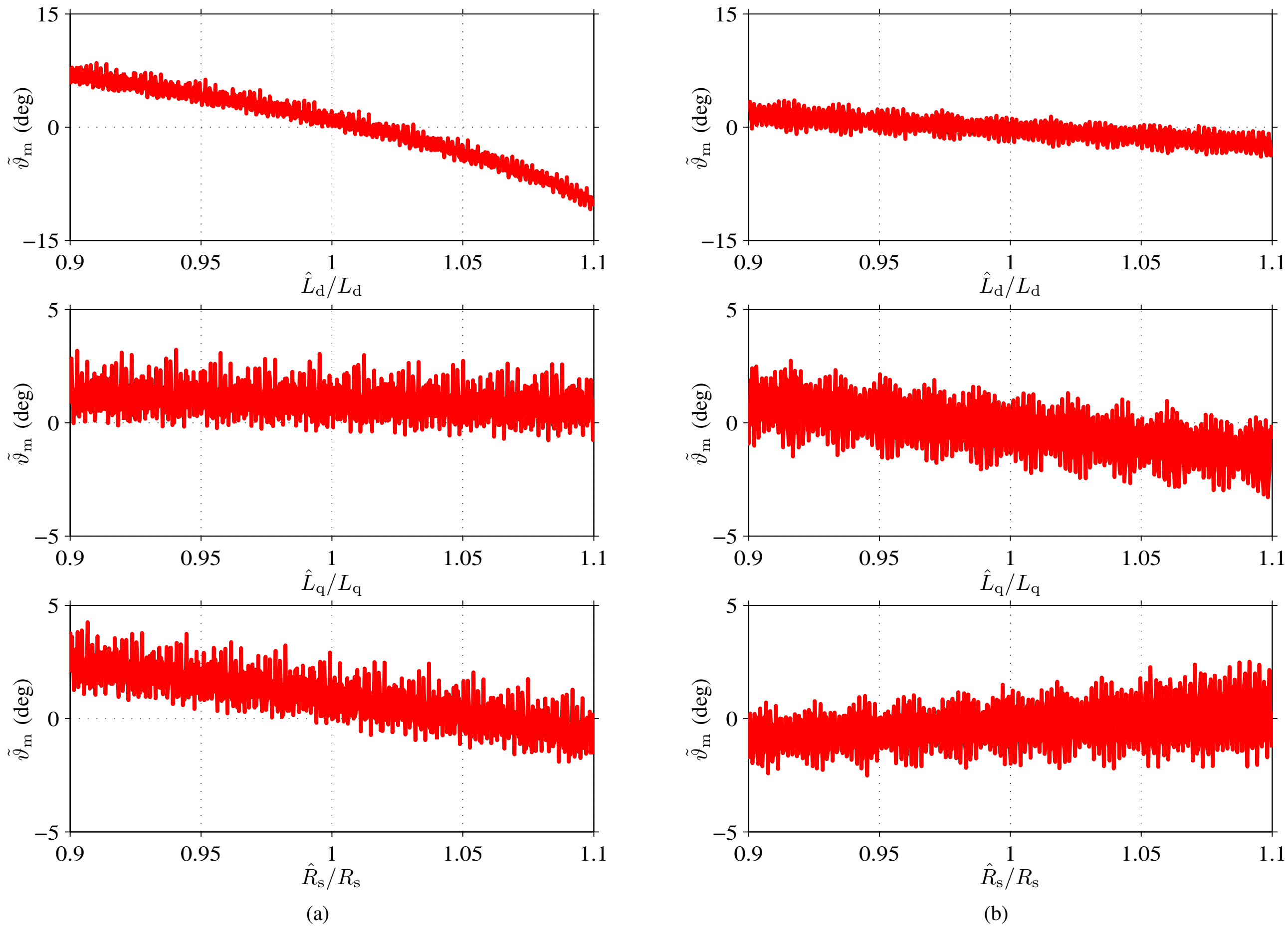

Fig. 1. Measured errors in the position estimate at $\hat{\omega}_{\mathrm{m}} = 0.1$ p.u. with 50% rated load torque applied: (a) reduced-order observer and (b) adaptive full-order observer. The data is captured by varying each model parameter from 90% up to 110% of the actual value in 10 seconds.

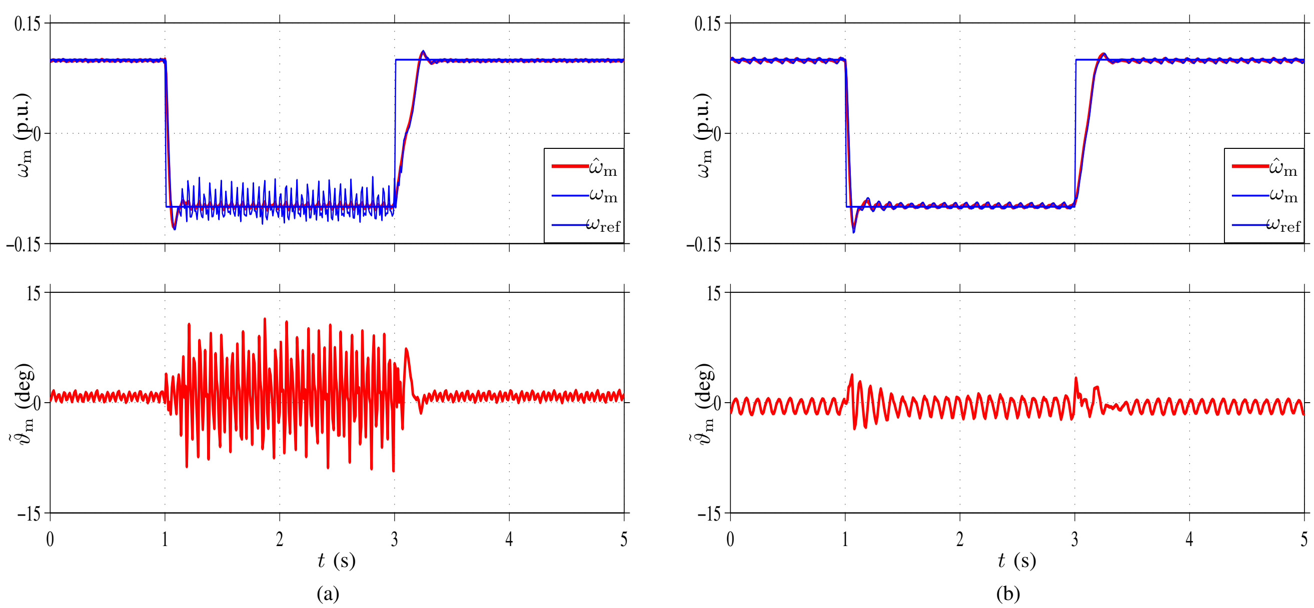

Fig. 2. Experimental results of a stepwise speed reversal (0.10 p.u. → −0.10 p.u. → 0.10 p.u.) with rated load torque applied: (a) reduced-order observer, (b) adaptive full-order observer.

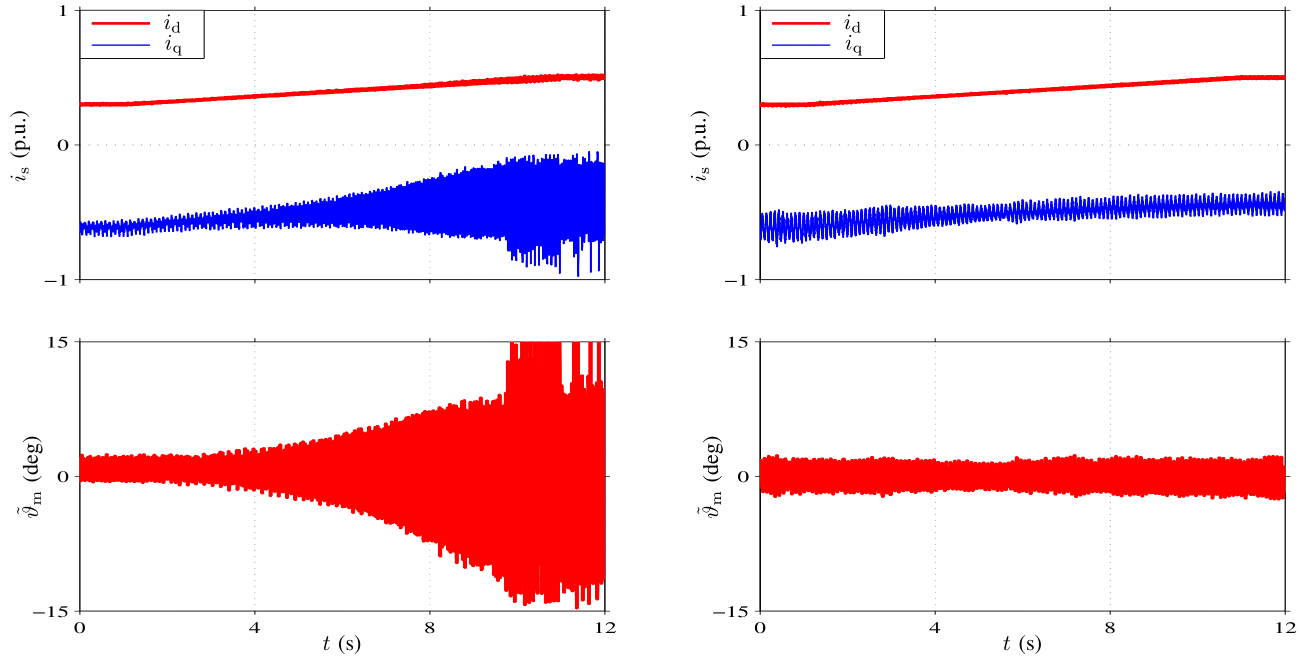

(a) (b)

Fig. 3. Experimental results of a slow change in i_d from 0.3 p.u. to 0.5 p.u. with −50% rated load torque applied: (a) reduced-order observer, (b) adaptive full-order observer.

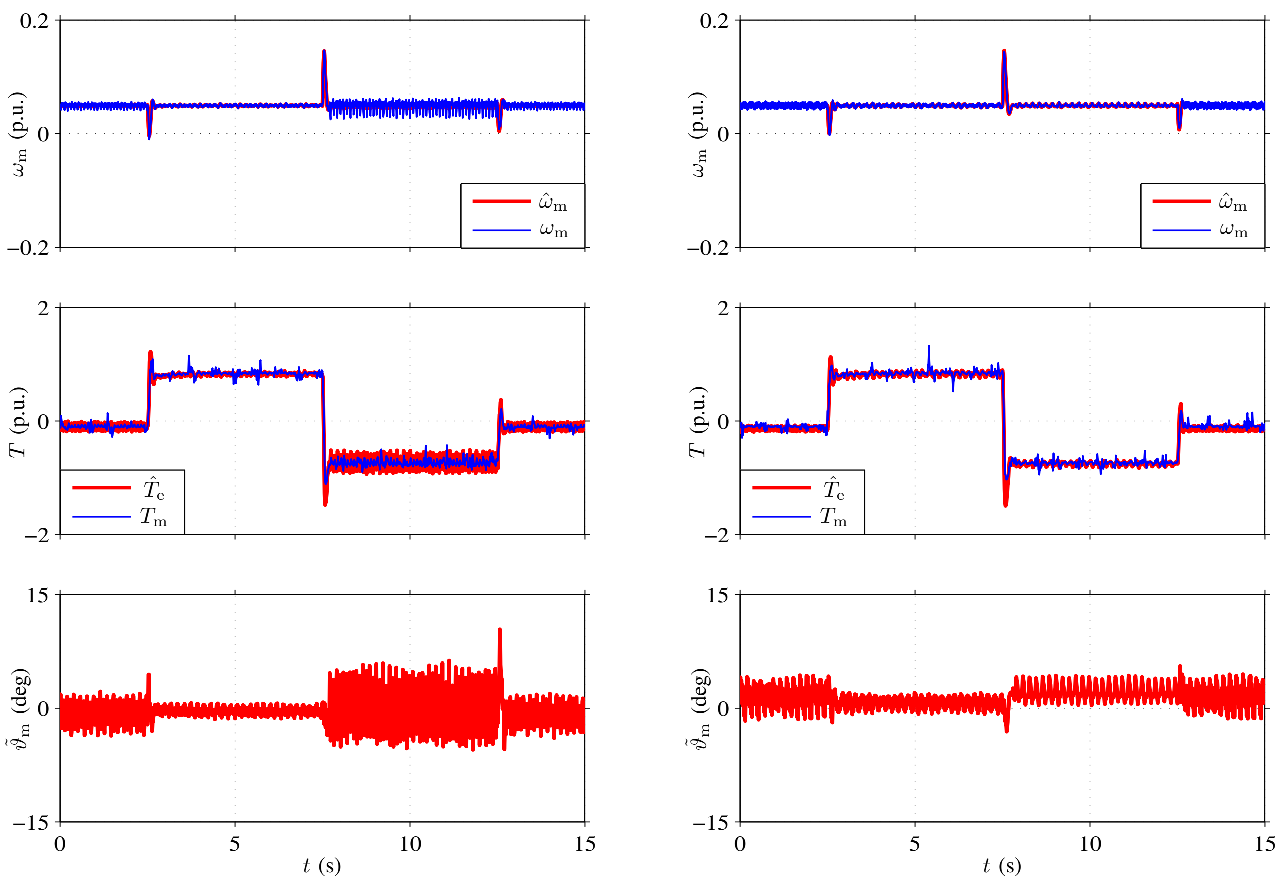

(a) (b)

Fig. 4. Experimental results showing load-torque steps (0 → −75% rated → 75% rated) when the speed reference is kept at 0.05 p.u.: (a) reduced-order observer, (b) adaptive full-order observer.